SURFACE TENSION DRIVEN CONVECTION EXPERIMENT-2 (STDCE-2)

Y. Kamotani[1], S. Ostrach[2] and J. Masud[3] [1,2,3] Department of Mechanical and Aerospace Engineering
Case Western Reserve University, Cleveland, Ohio 44106

INTRODUCTION

Thermocapillary flows are known to become oscillatory (time-periodic), but how and when they become oscillatory in containers of unit-order aspect ratio are not yet fully understood. The present work is a part of our continuous effort to obtain a better understanding of the phenomenon. Thermocapillary flow experiments in normal gravity are limited to a narrow parametric range in order to minimize gravity and buoyancy effects, which is an important reason for our lack of full understanding of the oscillation phenomenon. One important unanswered question is what role, if any, free surface deformation plays in the oscillation mechanism. For that reason we performed thermocapillary flow experiments, called the Surface Tension Driven Convection Experiment-2 (STDCE-2), aboard the USML-2 Spacelab in 1995. The main objectives of the experiments were to investigate oscillatory thermocapillary flows in microgravity and to clarify the importance of free surface deformation in such flows.

Steady and oscillatory thermocapillary flows were generated in cylindrical containers by employing two heating modes. A CO_2 laser with adjustable power and beam diameter was used in the Constant Flux (CF) configuration to heat the free surface. The other configuration investigated in STDCE-2 was the Constant Temperature (CT) configuration in which a submerged cylindrical cartridge heater placed at the symmetry (axial) axis of the test container heated the fluid. Both heating modes cause non-uniform temperature distributions on the free surface, which generates thermocapillary flow. The flow field was investigated by flow visualization, and the temperature field was measured by thermistors and an infrared imager. The free surface shape and motion were measured by a Ronchi system. The hardware performed well and we were able to conduct more tests than originally planned. From the successful experiments a large amount of data was acquired. The analysis of the data is now nearly complete. Some important results are presented and discussed herein.

DESCRIPTION OF EXPERIMENT
Experimental Apparatus

The experimental arrangement for STDCE-2 is sketched in Fig. 1. The objective of STDCE-2 was to investigate the onset conditions and nature of oscillatory flows under a variety of test conditions and
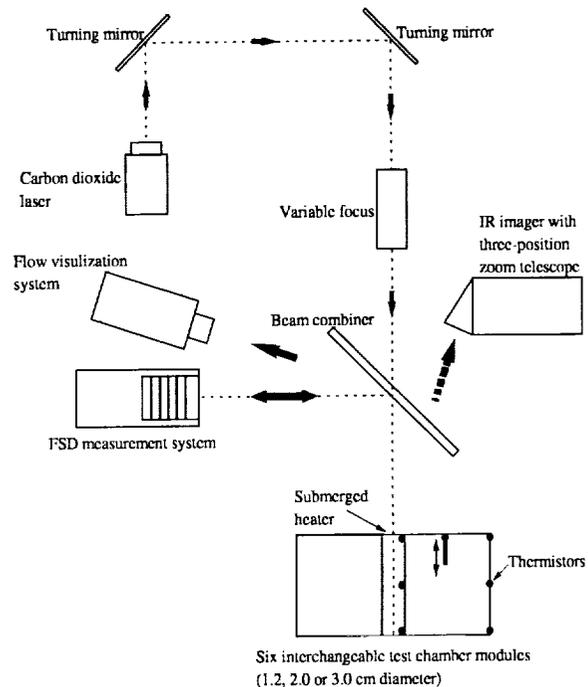
Figure 1. Schematic layout of STDCE-2.

configurations, including a study of the effect of heating mode, heating rate, surface heat flux distribution, container size and static free surface shape on the oscillations. Cylindrical test cells of various sizes (1.2, 2.0 and 3.0 cm diameter test cells), each with a nominal aspect ratio of one (radius=depth), were used. Silicone oil with kinematic viscosity of two centistokes was selected for use in STDCE-2. In the CF heating mode the laser power level and laser spot size could be varied to study the effects of heat input and surface heat flux distribution on the flow field. In the CT mode the cartridge heater power could be varied to study the effect of internal heat input and heater-to-external wall temperature gradients on the flow field. The static free surface shape of the test fluid was a variable in the STDCE-2 test matrix. Each test module contained an oil delivery system, which allowed the oil in the module's test cell to be filled to various levels. The free surface shapes in the STDCE-2 tests are shown in Fig. 2.

Each test chamber module consisted of an upper housing, a test section, a lower housing and an oil reservoir. The test section of each module consisted of

CF TEST CONTAINERS

SC =shallow concave, DC =deep concave

CT TEST CONTAINERS
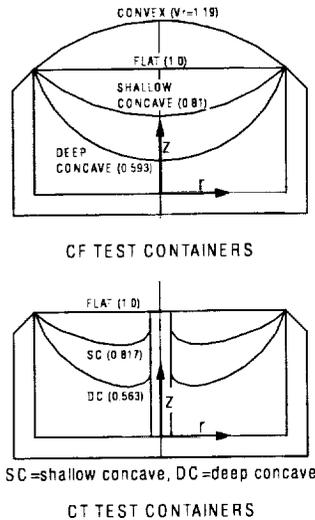
Figure 2. Free surface shapes in STDCE-2.

a high thermal conductivity, cylindrical, water-cooled copper test chamber wall with water cooled channels, a Teflon bottom, a movable thermistor, a central cartridge heater (for CT modules), an oil fill port, and a floor thermistor all held in place by an aluminum backing plate and bolts and sealed with an O-ring. The side walls were maintained at a nearly uniform temperature by circulating water. Each test chamber module included a reservoir containing a mixture of oil and tracer particles.

Temperatures were measured using thermistors positioned at various locations within and at the boundaries of the test cell (see Fig. 1). Side wall temperature was monitored at three locations. Bulk fluid temperature was measured using a movable thermistor which was translated by a thermistor crank external to the module. The movable thermistor could be precisely positioned parallel ($\pm$ 0.1 mm) to the axis of the test cell. All temperature measurements in the STDCE-2 tests were accurate within ±0.1 C with a response time of 0.1 seconds.

For the CT modules, a submerged, cylindrical electrical resistance heater (centered in the test cell) was used to heat the oil. These cartridge heaters were one-tenth the diameter (1.2, 2.0 and 3.0 mm) of the test chamber and extended the depth of the test cell from the pinning edge plane. Three thermistors were embedded in the heater's shell. The RF-excited CO_2 laser was used to heat the fluid surface during the CF tests at powers from 0.2 to 5.0 Watts, in 0.01 Watt increments, with all the energy absorbed within 0.2 mm of the surface. The optics were designed to produce heating zone sizes between 0.6-6 mm at the free surface for both curved and flat surface shapes.

A flow visualization system illuminated suspended 70 micrometer tracer particles (Pliolite) in the test fluid to provide a qualitative record of the bulk flow. In addition, this system was used extensively to monitor the flow for the onset of oscillations and the fluid behavior while filling the test cell. Laser diode was used for illumination for both flow visualization and free surface deformation measurement.

A scanning IR imaging system operating in the 8-14 micrometer wavelength range was used to detect radiated emissions to determine the thermal signature along the fluid free surface. The imager was identical to that used in the STDCE-1 experiments. A zoom telescope was fitted externally to the imager to properly focus to the three test cell sizes. New to STDCE-2 was a Ronchi interferometer, designed to measure the dynamic surface deformation during the experiment.

Ranges of Parameters

The important dimensionless parameters for steady thermocapillary flows in the present experimental configuration with a flat free surface are: Marangoni number $Ma = \sigma_T \Delta TR/\mu\alpha$, Prandtl number $Pr = \nu/\alpha$, aspect ratio $Ar = H/R$, and heater ratio $Hr = R_h/R$, where ΔT is the temperature difference between the heater and the side wall, R is the container radius, H is the depth, R_h is the heater radius, μ is the fluid dynamic viscosity, ν is the kinematic viscosity, α is the fluid thermal diffusivity, and σ_T is the temperature coefficient of surface tension. The Reynods number of the flow, $R\sigma$, can be computed as Ma/Pr. In addition, the relative fluid volume (Vr) is important in the curved surface tests and its value for each shape is given in Fig. 2. Based on numerical analysis, the heat loss from the free surface relative to the total heat transfer rate is estimated to be about 3 % so that it is not a major factor in the present experiments.

Forty two tests were performed in the CF mode. The parametric ranges of those CF tests were: $Ma < 6\times10^4$, $Pr = 22-32$, and $Hr = 0.05, 0.1$, and 0.2. 32 tests were conducted with $Ar = 1$. In the other 10 tests a cylindrical plastic disc was inserted at the bottom of each test chamber to reduce its aspect ratio to 0.5. The fluid viscosity in the above Pr is evaluated at the mean temperature, $(T_H + T_C)/2$, where T_H is the free surface temperature at the center. The above Ma is based on ΔT, which is convenient because Ma is defined similarly in other configurations. Later, a Ma based on Q will also be introduced. Ar and Hr in the thirteen CT tests were fixed at 1.0 and 0.1, respectively. The values of Pr and Ma in the CT tests were Pr=26-31 and Ma $\leq$ 1.7×10^5.

RESULTS AND DISCUSSION
Oscillatory Flow in CT Configuration

It is known from our previous studies[1,2] in the CT configuration that once ΔT is increased beyond a certain value (called the ΔT_{cr} herein), the flow field becomes oscillatory with corresponding time periodic variations in the temperature field. The onset of oscillatory flow disturbs the axial symmetry of the flow and temperature fields which then become three dimensional and periodic in time. The observed oscillatory motion in all the tests in STDCE-2 was similar in nature. In oscillatory flow, the fluid particles moved back and forth in the azimuthal direction with the frequency of oscillations as they circulated in the flow cell. In addition to the oscillatory motion in the azimuthal direction, a very slow rotation of the whole flow field was also observed. The time period of this rotation was much larger than the time period of the oscillatory motion in the azimuthal direction. In a fixed radial (r-z) plane (see Fig. 2), the flow was observed to go through periods of strong and weak motion during one oscillatory cycle. The observed oscillatory flow field is similar to that described by Kamotani et al.[1,2] in 1-g tests

The onset of oscillatory flow is signified by ΔT_{cr} which is shown in Fig. 3 for various test containers with flat free surface. 1-g data from Kamotani et
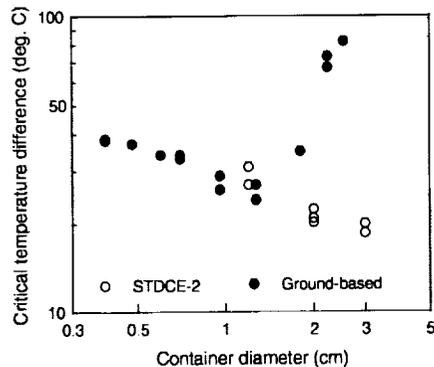
Figure 3. Critical temperature differences for CT tests.

al.[1] for the CT configuration (same fluid and Hr as in the STDCE-2 tests) are also included to increase the range so as to make the trend clear. It can be seen that the data taken in normal gravity exhibit two different trends: ΔT_{cr} decreases gradually with increasing container diameter (D) up to about D=1.2 cm and then increases sharply beyond that. For the test containers with diameter around 1.2 cm, the onset of oscillations in 1-g and microgravity occur at a similar ΔT_{cr}. The small difference in ΔT_{cr} noticeable from Fig. 3 is due

to a somewhat different cold wall temperature in the 1-g ($\sim$25 °C) and microgravity ($\sim$15 °C) experiments, which results in slightly higher viscosity in the microgravity tests for the same fluid. For the test containers with 1.2 cm diameter, in addition to the similarity in the observed oscillatory flow field, the oscillation frequency and the IR image of the free surface were also similar in the 1-g and microgravity tests. This clearly shows that for the 1.2 cm diameter test container, buoyancy does not influence the onset of oscillations. Therefore, one can conclude that the onset of oscillations in test containers with diameter smaller than 1.2 cm is not affected by buoyancy in normal gravity as the influence of buoyancy is reduced with decreasing test container dimensions. Then, in the absence of buoyancy it can be seen from Fig. 3 that ΔT_{cr} decreases with increasing test section size.

In order to determine the criteria for the onset of oscillations, it is appropriate to look at the problem in a nondimensional manner. The important factors which could influence the onset of oscillations in the absence of buoyancy are: Ma, Pr, Hr, Ar, heat loss from the free surface and the deformability of the free surface. In the present experiments, the heat loss from the free surface is estimated numerically and is found to be insignificant for the conditions near the onset of oscillations. Therefore, if the free surface is assumed to be nondeformable, then the conditions of the experiment are determined by Pr, Ar, Hr and Ma. In the present experiments Ar and Hr are fixed and Pr is nearly constant in all the tests, therefore, the only variable parameter is Ma. Consequently, the onset of oscillations should be characterized by a critical Marangoni number (Ma_{cr}). In order to see the behavior of Ma_{cr} in the present and in our 1-g experiments, the data in Fig. 3 (1-g data for D$\leq$1.2 cm) are nondimensionalized in terms of Ma_{cr} and plotted in Fig. 4 against the test container diameter to differentiate among various tests. From Fig. 4 it is clearly seen
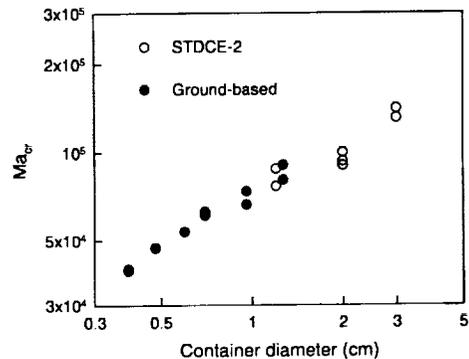
Figure 4. Critical Marangoni numbers for CT tests.

that for different tests with similar Pr, Ar and Hr, the value of Ma_{cr} changes almost fourfold over the range of the experiments. This shows that Ma_{cr} is not a sufficient parameter to characterize the onset of oscillations in the CT configuration. The same conclusion was obtained in our previous work in other configurations.

It is clear then that some other factor needs to be included in the analysis. Since buoyancy and heat loss from the free surface are insignificant, the only important factor is the deformability of the free surface. Based on our extensive experimental and theoretical work on the oscillation phenomenon, we believe that the additional aspect is free surface deformation. The detailed theoretical basis for oscillatory thermocapillary flows in the so-called half-zone configuration is given by Kamotani et al.[3] The same concept is applied to the present configuration. It is convenient to divide the flow field into two: surface flow along the free surface toward the cold wall and return flow in the interior toward the heated region. The surface flow is driven by thermocapillarity and the return flow is due to the pressure field caused by the surface flow. Consider a transient situation where the surface flow is somewhat changed for some reason. The return flow does not respond to that change immediately, because the surface flow must deform the free surface shape first to modify the pressure field. Such a small delay could cause a large change in the flow field, if the free surface deformation alters the thermal boundary layer thickness along the free surface significantly.

It can be shown that the amount of transient free surface deformation relative to the thermal boundary layer thickness in the hot corner (the region next to the heater where the surface temperature gradient is large) can be expressed as

$$\left(\frac{\rho \alpha^2}{R\sigma} \right)^{1/2} Ma \equiv S \qquad (1)$$

where σ is the surface tension. The above parameter is called a surface deformation parameter or S-parameter. According to our oscillation model, the oscillation process could start when the S-parameter becomes larger than a certain finite number. The critical conditions are plotted in terms of Ma and S in Fig. 5 As the figure shows, all the data can be correlated well by S: The flow becomes oscillatory when S is larger than about 15.

According to our oscillation model, the oscillation period (1/f) scales with the time of convection along the heater surface. Based on that, the dimensionless oscillation frequency (f*) is defined as

$$f^* \equiv \left(\frac{fR^2}{\alpha} \right) Ma^{-2/5} \qquad (2)$$

The dimensionless frequencies measured in STDCE-2 and in our ground-based tests with small containers are plotted against
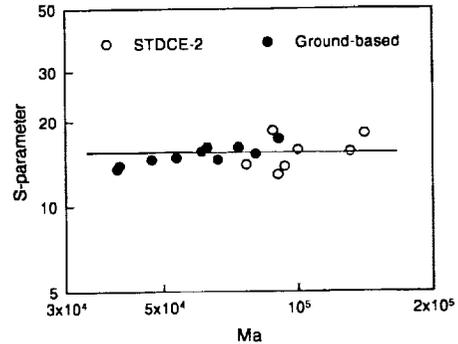
Figure 5. Critical S-parameter for CT tests.

Ma in Fig. 6. The dimensionless frequency is nearly constant, equal to about 1.8, in all the tests, consistent with the scaling law of Eq. (2).
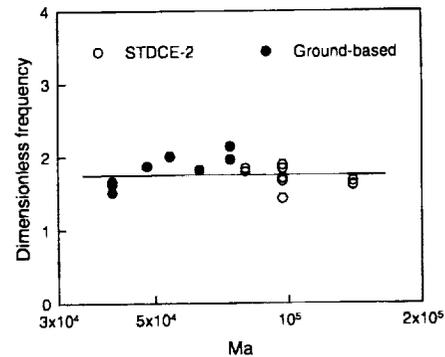
Figure 6. Dimensionless oscillation frequencies for CT tests.

Oscillatory Flow in CF Configuration

The oscillatory flow structure in the CF configuration was similar to that in the CT configuration. The heat input at the onset of oscillations is called critical heat flux (Q_{cr}). The critical heat fluxes measured in the flat surface tests with Ar = 1 are presented in Fig. 7, together with data taken in our ground-based tests with smaller containers filled with the same fluid (Lee et al.[4]). The flow was found to be already oscillating at the minimum power of the CO_2 laser for the 1.2 cm container, so that the critical heat flux could not be determined for that container. As seen in Fig. 7, trend of the space data is consistent with that of the ground data: Q_{cr} increases with increasing D. According to Fig. 7, Q_{cr} seems to depend slightly on Hr but the effect of Hr is within the experimental error.

It can be shown from scaling and numerical analyses (Kamotani et al.[5]) that the steady flow in the CF

266
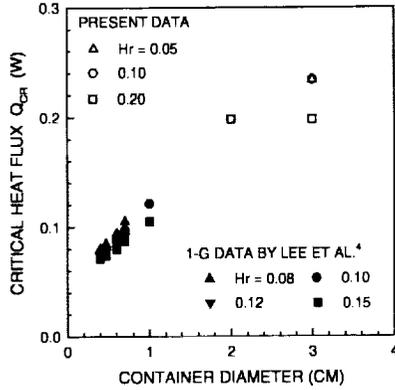
Figure 7. Critical heat fluxes in CF tests.

configuration is driven mainly in the bulk region outside the heated region. Then, it is appropriate to use the following Marangoni number based on Q,

$$Ma_Q = \left(\frac{\sigma_T Q}{k\mu\alpha}\right)^{2/3} \tag{3}$$

Based on the critical heat flux for onset of oscillations, we compute $(Ma_Q)_{cr}$ according to Eq. (3). The result is given in Fig. 8, where we plot $(Ma_Q)_{cr}$ against D, since D is the only main quantity varied in those tests. If $(Ma_Q)_{cr}$ is the only parameter to specify onset of oscillations, it should not vary with D. Figure 8 shows that, as we have found also in various other experiments under different conditions, including the CT tests in STDCE-2, the critical Marangoni number varies with container size. Clearly, Ma alone cannot specify the onset.
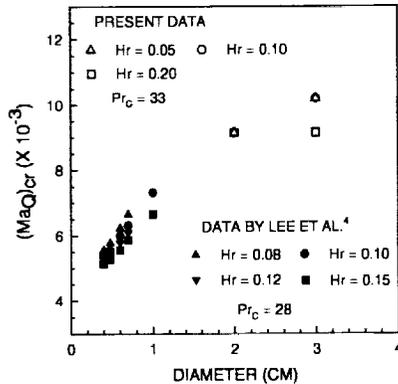
Figure 8. Critical Marangoni numbers for CF tests.

As in the case of CT configuration, free surface deformation plays an important role in the oscillation mechanism, as explained in Kamotani et al.[5] The ratio of free surface deformation in the heated region to the thermal boundary layer thickness is called S-parameter as before, and it can be shown that the S-parameter in

the CF configuration can be expressed as (Kamotani et al.[5])

$$S = \left(\frac{\rho\alpha^2}{\sigma R}\right)^{1/2} Ma_Q^{11/8} Pr^{1/8} \tag{4}$$

The data in Fig. 8 are replotted in Fig. 9 where S is
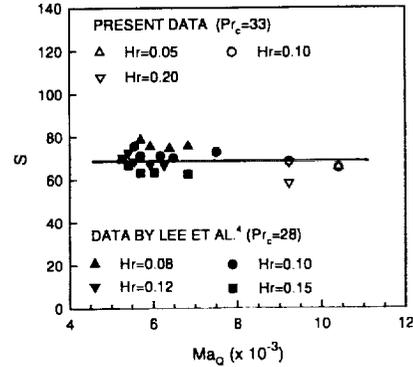
Figure 9. Critical S-parameter for CF tests.

computed according to equation (4). As seen in the figure, all the data are correlated very well with the S-parameter: all the data lie within S = 69 ± 14%. The data scatter is largely due to the effect of absorption length. Therefore, one can say that the flow becomes oscillatory when S is larger than about 70. It is clear that Ma_Q is an important parameter, because the oscillations are a convection phenomenon, but in the parametric ranges of STDCE-2 and our ground tests the S-parameter is the limiting parameter.

The frequency of oscillations are shown in Fig. 10. Only a few data are available from our ground-based tests. Except for the data for D = 1.2 cm, the oscillations frequencies were obtained near the onset of oscillations. The frequency decreases with increasing D. The frequency is not a strong function of Hr. As in the CT configuration, the oscillation period scales with the time of convection, based on which the oscillation frequency is non-dimensionalized herein as (Kamotani et al.[5])

$$f^* = \left(\frac{fR^2}{\alpha}\right)/Ma_Q \tag{5}$$

The dimensionless frequencies are presented in Fig. 10. The figure shows that f* is nearly constant (about 0.018) in agreement with Eq. (5). The values for D = 1.2 cm are generally smaller than those for other containers, which is due to the fact that the oscillatory flow was not close to the onset.

267
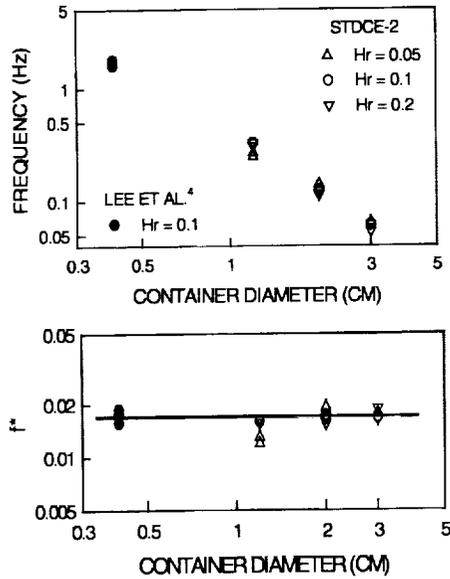
Figure 10. Dimensional and dimensionless oscillation frequencies for CF tests.

SUMMARY

The Surface Tension Driven Convection Experiment-2 (STDCE-2) was conducted aboard the USML-2 Spacelab in 1995 to study oscillatory thermocapillary flows. The STDCE-2 completed all of its defined tests for the mission, several re-run tests to check data reproducibility, and additional tests with shallow test chambers. In all, 42 constant flux tests and 13 constant temperature tests were conducted and completed successfully, and oscillations were found in most of the tests. The hardware performed very well, and the quality of the video and digital data was excellent. Only some important data taken in the STDCE-2 tests are presented and discussed herein. The most important finding is that the Marangoni number cannot specify the onset of oscillations, which suggests that free surface deformation plays an important role. Based on the physical model of oscillations, we introduce a surface deformation parameter, which represents the ratio of transient free surface deformation to thermal boundary layer thickness in the heated region. The parameter correlates the STDCE-2 and our ground-based data well.

ACKNOWLEDGMENTS

REFERENCES

[1]Kamotani, Y., Masud, J., and Pline, A., "Oscillatory Convection Due to Combined Buoyancy and Thermo-capillarity" J. Thermophysics & Heat Transfer, Vol.10, No.1, pp.102-108, (1996).

[2]Kamotani, Y., Lee J. H., Ostrach, S., and Pline, A., "An Experimental Study of Oscillatory Thermocapillary Convection in Cylindrical Containers" Physics of Fluids A, Vol.4, No.5, pp.955-962, (1992).

[3]Kamotani, Y. and Ostrach, S., "Theoretical Analysis of Thermocapillary Flow in Cylindrical Columns of High Prandtl Number Fluids," accepted for publication in Journal of Heat Transfer, 1998.

[4]Lee, J. H., Ostrach, S., and Kamotani, Y., "A Study of Oscillatory Thermocapillary Convection in Circular Containers with CO_2 Laser Heating," Report EMAE/TR-94-213, Department of Mechanical and Aerospace Engineering, Case Western Reserve University, Cleveland, OH. (1994).

[5]Kamotani, Y., Ostrach, S., and Masud, J., "Oscillatory Thermocapillary Flows in Open Cylindrical Containers Induced by CO_2 Laser Heating," accepted for publication in International Journal of Heat and Mass Transfer, 1998.